IRANIAN JOURNAL OF CATALYSIS

Sonosynthesis, characterization and photocatalytic degradation property of nanoZnO/zeoliteA

Shokufeh Aghabeygi*, Reza Kia Kojoori, Hamideh Vakili Azad

Department of Chemistry, East Tehran Branch, Islamic Azad University, Tehran, Iran.

ABSTRACT

Nano hexagonal wurtzite ZnO has been prepared on zeoliteA by the sono-chemical method. The zeoliteA was mixed into Zinc gel, after stirring for two days, the mixture was irradiated 30 min by ultrasonic probe. The filtrated composite gel was calcinated at 500°C for 3h in furnace. The produced composite was characterized using X-ray diffraction, FT-IR spectroscopy and field emission scanning electron microscopy. The average crystal size of the nanoZnO and nanoZnO on zeoliteA was determined 53 and 38 nm, respectively. The range of particles size of the nanoZnO on zeoliteA is 30-50 nm. The particles of nanoZnO on the surface of zeoliteA has been dispersed over the zeoliteA framework and the results have shown a higher rate of photodegradation of Congo red (an azo-dye) as compared with bare nanoZnO.

Keywords: ZeoliteA, Ultrasonic, NanoZnO, Photocatalyst, Congo red.

1. Introduction

Nano-sized semiconductor particles can be more active in the photo-catalysis than films and micro-particles. [1,2]. ZnO as the well-known semiconductor has been intensively investigated in the fields of photo-catalysis, solar cell and gas sensors due to their special electronic and optical properties [3-6]. Semiconductors, such as ZnO, play the most promising roles in several areas of research. The ZnO/Air/ UV system is the most effective one. The heterogeneous photo-catalytic behavior of ZnO under UV irradiation, which leads to the generation of electron and hole pairs at conduction and valence bands, respectively, has been studied extensively [4–9]. ZnO, as a semiconductor, is also usually used as photocatalyst to destroy the organic pollutants in water because its high photo-sensitivity and large band gap can offer the high driving force for reduction and oxidation processes. It has been proved that ZnO may exhibit a better efficiency than TiO_2 in photocatalytic degradation for some dyes [10-13]. Intense research has also been conducted on the effect of ZnO particle size on its photo-catalytic activity. It is well known that in the nano-meter size range, the physical and chemical properties of the semiconductor are found to be modified as compared with those of the bulk semiconductor. Decrease in the size of the particles causes an increase in the photo-catalytic activity of the semiconductor. Therefore, control of the size, to which particles grow in, a nano-meter range, becomes necessary [14-16]. One strategy to obtain ZnO with defined particle size can be the use of various supports such as silica, zeolite, clay, etc, and dispersal of the catalyst particles on them [17–19]. High extensive surface area, high adsorption capacity and charged framework have made zeoliteA one of the most suitable supports [20-23]. Zinc oxide is a II–VI group, n-type direct band gap semiconductor that possesses some great characteristics, including a wide energy band gap (3.3 eV) [24,25].

In this research, we synthesized the high dispersed nanoZnO over the zeoliteA as a composite with high surface area by sono-chemical method. Sono-synthesis is one of the best methods to decrease the particle size. To investigate the photo-catalytic activity of the nanoZnO/zeoliteA composite, the catalyst was used in degradation of Congo red, an azo-dye, under UV irradiation at the λ max of the dye (502nm). In this research, we intend to emphasize the advantages of synthesizing nanoZnO on zeoliteA with high surface area by sono-chemical method as compared with bare ZnO and impregnated ZnO.

---

*Corresponding author email: saghabeygi@yahoo.com
Tel: +98 21 3359 4950; Fax: +98 21 3358 4011

2. Experimental

2.1. Materials

All the chemical reagents used in this research were analytical grade and without further purification. Deionized water (DI) was used in all experiments.

### 2.2. Sono- synthesis of Nano ZnO/ZeoliteA composite

For preparation of ZnO gel, 4.4 g $Zn(CH_3COO)_2.2H_2O$ was firstly dissolved in DI water (100 ml) and stirred to get a precursor solution, the 20 ml (2M) NH_3 (aq) was dropped into the precursor solution, one drop per second, until pH of mixture was adjusted 9 during stirred solution, and the white suspension of $Zn(OH)_2$ appeared.

$Zn(CH_3COO)_2$ + 2 NH_3(aq) $\longrightarrow$ $Zn(OH)_2$ + 2NH_4 CH_3COO
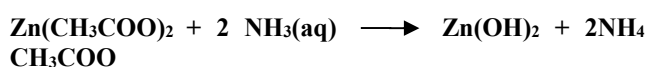
The zeoliteA was directly incorporated into the ZnO gel to get the ZnO/zeoliteA composite gel. As aging time, the mixture of reaction was continuously stirred for two days. The solution was sonicated by an Ultrasound Horn (Bandelin, SONOPULS 20 kHz) at 85% amplitude delivering power of 200W by the Titanium flat tip of probe for 30 min with 0.5 s pulse and 0.5 s silent period cycles to achieve a ZnO/zeoliteA homogenous gel. After filtering, the prepared white powder of nanoZnO/zeoliteA was calcinated in furnace at 500°C for 3h [26,27].

2.3. Photodegradation process

In order to test the photocatalytic activity of the nanoZnO/zeoliteA, we chose Congo red (CR) as a model of water pollution to evaluate the catalytic behavior of the samples (Fig. 1).
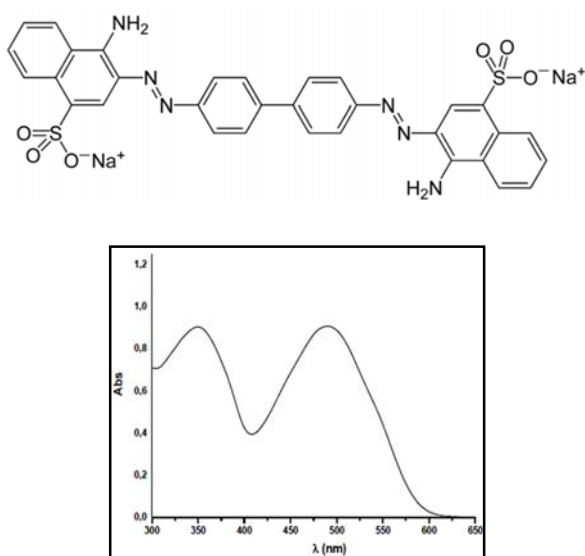
Fig.1. Structural formula and UV-Vis spectrum of Congo red $C_{32}H_{22}N_6Na_2O_6S_2$.

Photodegradation of 10 parts per million (ppm) CR solution was used to evaluate the performance of nanoZnO and nanoZnO/zeoliteA composite photocatalysts. For each condition, 0.05 g of photocatalyst was dispersed into 100 ml of 10 ppm CR aqueous solution. The CR solution was placed on a magnetic stirrer plate and a stirrer bar placed in it for stirring of the particles throughout the experiment.

The photo-catalytic reaction was conducted at room temperature under UV light from a single 15W UV tube at 254 nm positioned horizontally above the liquid surface. The distance between the lamp and the base of the beaker was 10 cm. Each experiment was conducted for 2 h with 5ml sample aliquots extracted every 15 min. The decomposition of CR was monitored by measuring the absorbance of the aliquot solution at 502 nm (λ_{max} of CR) using the UV–Vis spectrophotometer (U-3010, HITACHI). The photo-catalytic degradation (PD) was calculated by the following formula:

$$\%PD = \left[\frac{Ao - At}{Ao}\right] \times 100$$

Where Ao is the initial absorbance of CR solution, which reached absorbency balance and At is the absorbance of the dye solution at irradiation time (t).

2.4. Characterization

The IR spectra were performed as KBr disks on a Bruker Tensor 27 FT-IR spectrometer. XRD measurements were performed using an X'pert diffractometer (Philips Company) with monochromatized Cu-Kα radiation (λ = 1.54056 Å). The samples were characterized with a FESEM (Hitachi S4160 (Cold Field Emission) with gold coating.

3. Results and Discussion

3.1. FT-IR spectra

The FT-IR spectra of nanoZnO/zeoliteA composite and pure nanoZnO (wurtzite) are shown in Fig. 2. The wide peaks at 3500-3000 cm^{-1} were assigned to the OH symmetry and asymmetry stretching vibration of water molecule. The peaks at about 1630 cm^{-1} resulted from bending vibration of the adsorbed H_2O molecules, which were not removed completely after sol–gel synthesis. As shown in Fig 2b, the water molecules were trapped in zeoliteA pores, therefore, the peaks of water vibrations in Fig 2b are larger than nanoZnO (Fig 2a). The peaks at 1142, 1064 and 911cm^{-1} have resulted in bending and stretching vibration of, O-Si-O bonds and Al-O-Si of zeoliteA. The peaks at 671, 609 and 572 cm^{-1} have been related to the bending and stretching of the Zn-O-Zn bonds and flexion. The peaks at 410, 459 and 505 cm^{-1} can been attributed to T–O bending vibrations and double ring vibrations of zeoliteA, respectively. [28]
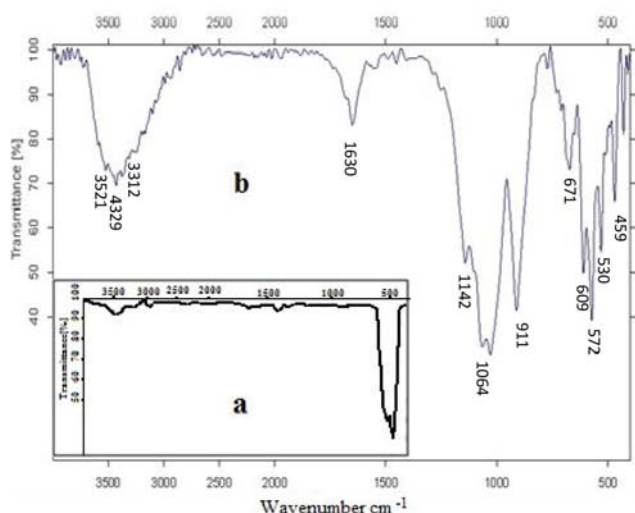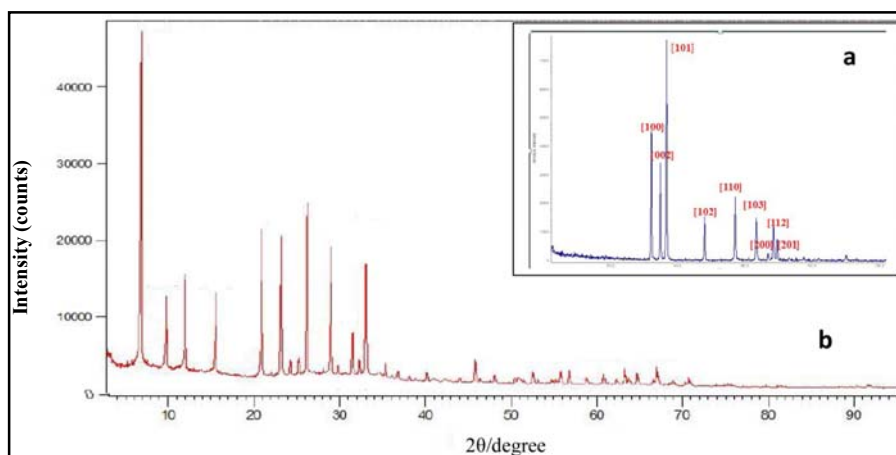
Fig. 2. FT-IR spectra of (a) nanoZnO and (b) nanoZnO/zeoliteA composite.

3.2. XRD pattern

Fig. 3a and b present the XRD patterns of the sono-synthesized nanoZnO hexagonal wurtzite and nanoZnO on zeoliteA. In Fig. 3a, the peaks indicate the respective joint committee on powder diffraction standards (JCPDS) card No. 36–1451, for hexagonal wurtzite structure of ZnO. In Fig. 3b, the diffraction peaks appear at 2 θ, 7.0, 10.0, 12.5, 14.5, 16.1, 21.8, 23.24, 27.1 and 30.0, 31.0, 32.5 and 34.2 are related to the zeoliteA. These values of 2θ are observed that have a good agreement with the data of Na-A zeolite in the library of the instrument (card No 38–0241) and in the literature [22]. The average crystallite size of samples **Dv** was calculated based upon the XRD pattern for the quantitative purpose using the Debye-Scherer equation [23,29]:

$$Dv = \frac{K\lambda}{\beta \cos \theta}$$

where Dv is the "volume weighted" crystallite size= ¾ d (crystallite diameter) K is the "Scherer constant" (around 0.89), λ is the wavelength of the X-rays here is λ, CuKα= 1.541 Å, θ is the Bragg angle for the peak at 2θ, β is the "integral breadth" of the peak at 2θ. The β= (π/2) FWHM (full width at half maximum) for a Gaussian shaped peak. According to XRD patterns, the mean crystallite sizes of nanoZnO and nanoZnO on zeoliteA are estimated to be 53 and 38 nm, respectively.

3.3. FESEM images

Fig. 4 shows the FESEM images of the nanoZnO and nanoZnO/zeoliteA composite, where the small particles located on zeoliteA crystals are those of nanoZnO. The ZnO nanoparticles might be located on the inner surface of zeoliteA. Surface and particle morphology of the synthesized nanoZnO and nanoZnO/zeoliteA composite have been studied and their FESEM images are shown in Fig. 4a and 4b, respectively. In the Figs., the small particles located on zeoliteA crystals are those of nanoZnO. The particle size of nanoZnO and nanoZnO over the zeoliteA is in the range between 60-90 nm and 30-50 nm, respectively.

3.4. Photodegradation of Congo red

The results of the absorbance of Congo red solutions are shown in Fig.5, where the efficiency of the dye removal is plotted against the UV irradiation time, using different catalysts.

In Fig. 6, the blank experiment without any catalyst under UV irradiation was rarely decomposed with less 10% degradation of CR.

In the second instance, for zeoliteA/UV system, the decolorization was due adsorption of dye molecules on the surface of zeoliteA and to the degradation ability of UV irradiation.
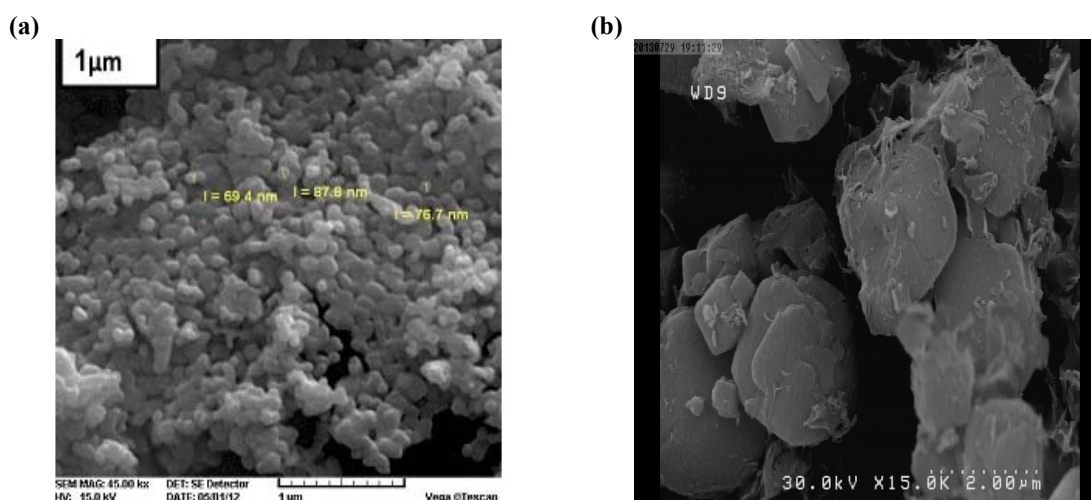

Fig. 3. XRD patterns of (a) nanoZnO and (b) nanoZnO/zeoliteA composite.

(a)

(b)

Fig. 4. FESEM images of (a) nanoZnO and (b) nanoZnO/zeoliteA composite.

In the third instance, a nanoZnO/UV system was tested less than 60% degradation of CR after 120 min. In the last instance, we used the synthesized catalyst (nanoZnO/zeoliteA composite) with which the most efficiency of degradation of CR was observed on the nanoZnO/zeoliteA-composites more than 92% after 2h under UV irradiation.

Furthermore, the strong electrostatic field present in the zeoliteA framework can effectively separate the electrons and holes produced during photo-excitation of nanoZnO and so resulted in lower recombination of them and higher photo-degradation efficiency.

After 30 minute of reaction, the degradation rate of the dye has decreased for all catalysts. The reason is that the surfaces of catalysts are covered by dye molecules. The nanoZnO/zeoliteA catalyst has shown the best results in photodegradation processes as compared with bare nanoZnO. The reason is that the gel prepared before the crystallization step has more flexibility, thus it can enter and disperse in all channels and pores of zeoliteA homogeneously, and the crystallization process occurs inside the pores and over the zeoliteA, which act as micro or nano-reactors [27,28].
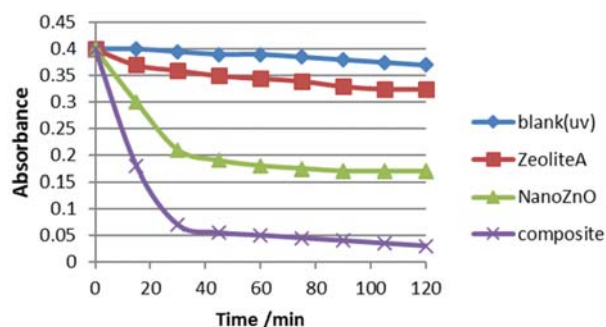
4. Conclusions

Synthesis of nanoZnO/zeoliteA composite by the sono-chemical method was done successfully. The (nanoZnO/zeoliteA/UV) process is proved to be a more successful method of photodegradation process than (zeoliteA/UV) and (nanoZnO/UV). The results of this investigation indicate that the adsorption property of this composite increases the photo-catalytic degradation efficiency of the dye. The structure of the zeoliteA with its channels and pores creates an extended area for dispersing of nanoZnO and this prevents the aggregation of the particles. Therefore, a large number of the dye molecules can absorb on the nanoZnO/zeoliteA particles, which can easily transfer the photogenerated electron and holes in the conduction and valence bands of ZnO, respectively. So, the rate and efficiency of degradation of Congo red becomes much higher as compared with the bare nanoZnO.

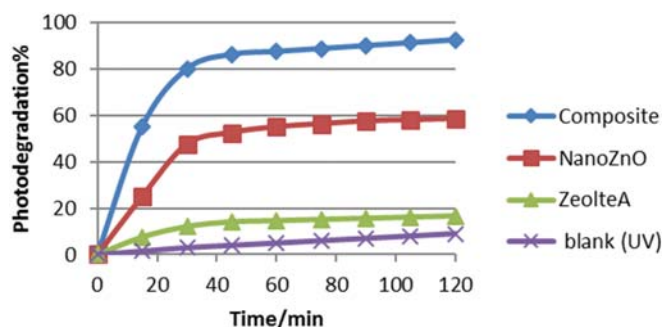**Fig. 5.** Plot of absorbance of CR solution versus reaction time.

Fig. 6. Plot of photodegradation of CR solution versus reaction time.

References

[1] G. Guan, T. Kida, K. Kusakabe, K. Kimura, E. Abe, A. Yoshida, Inorg. Chem. Commun. 7 (2004) 618-620.

[2] V. Yu, F. Meteleva, G.F. Roessner, Novikov, J. Photochem. Photobiol. A. 196 (2008) 154–158.

[3] Q. Zhang, C.S. Dandeneau, X. Zhou, G. Cao, Adv. Mater. 21 (2009) 4087–4108.

[4] J. H. Pan, H. Dou, Z. Xiong, C. Xu, J. Ma, X. S. Zhao, J. Mater. Chem. 20 (2010) 4512-4528.

[5] H.M. Xiong, J. Mater. Chem. 20 (2010) 4251–4262.

[6] G. Yang, Z. Yanb, T. Xiao, Appl. Surf. Sci. 258 (2012) 8704–8712.

[7] G. Zhou, J. Deng, Mater. Sci. Semicond. Process. 10 (2007) 90–96.

[8] B. Khodadadi, M. Bordbar, Iran. J. Catal. 6 (2016) 37-42.

[9] C.G. Silva, J. Monteiro, R.R.N. Marques, A.M.T. Silva, C. Martínez, M. Canle, J.L. Faria, Photochem. Photobiol. Sci. 12 (2013) 638–644.

[10] K. Gouvea, F. Wypych, S.G. Moraes, N. Duran, N. Nagata, P. Peralta-Zamora, Chemosphere 40 (2000) 433-440.

[11] B. Dindar, S. Icli, J. Photochem. Photobiol. A: Chem. 140 (2001) 263-268.

[12] D. Fu, G. Han, Y. Chang, J. Dong, Mater. Chem. Phys. 132 (2012) 673–681.

[13] A. Nezamzadeh-Ejhieh, M. Bahrami, Des. Water Treat. 55 (2015) 1096–1104.

[14] M. Anpo, T. Shima, Kodamas, Y. Kubokawa, J. Phys. Chem. 91 (1987) 4305–4310.

[15] V. Murugesan, L.S. Sakthive, M.V. Shankar, M. Palanichany, B. Arabindoo. J. Photochem. Photobiol. A 148 (2002) 153–159.

[16] C.W. Tang, Mod. Res. Catal. 02 (2013) 19–24.

[17] L. Vafayi, S. Gharibe, Iran. J. Catal. 5 (2015) 365-371.

[18] S. Danwittayakul, M. Jaisai, T. Koottatep, J. Dutta, Ind. Eng. Chem. Res. 52 (2013) 13629-13636.

[19] H.B. Hadjltaief, M.B. Zina, M.E. Galvez, P.D. Costa, J. Photochem. Photobiol. A 315(2016) 25-33.

[20] R.M. Mohamed, A.A. Ismail, I. Othman, I.A. Ibrahim, J. Mol. Catal. A: Chem. 238 (2005) 151-157.

[21] A. Nezamzadeh-Ejhieh, S. Khorsandi, J. Ind. Eng. Chem. 20 (2014)937-946.

[22] L. Zhao, Z.C. Liu, Z. F. Liu, Synth. Mater. Tech. 30 (2015) 60-64.

[23] A. Nezamzadeh-Ejhieh, Z. Banan, Desalination 284 (2012) 157–166.

[24] J.H. Lee, K.H. Ko, B.O. Park, J. Cryst. Growth 247 (2003) 119-125.

[25] C-Y. Tsay, K-S Fan, S-H Chen, C-H Tsai, J. Alloys Compd. 495 (2010) 126–130.

[26] M.R. Vaezi, J. Mater. Process. Technol. 205 (2008) 332–337.

[27] M. Khatamian, S. Hashemian, S. Sabaee, Mater. Sci. Semicond. Process 13 (2010) 156–161.

[28] L.J. Wang, Y. Chang, J.S. Li, Y.C. Yang, X.Y. Sun, Mater. Lett. 59 (2005) 3427–3430.

[29] Standard methods for the examination of water and wastewater, 18th ed., American Public Health Association, Washington D.C., 1992.